

Cannabinoid Receptor 1 Blockade Ameliorates Albuminuria in Experimental Diabetic Nephropathy

Federica Barutta,¹ Alessandro Corbelli,^{2,3} Raffaella Mastrocola,¹ Roberto Gambino,¹ Vincenzo Di Marzo,⁴ Silvia Pinach,¹ Maria Pia Rastaldi,² Paolo Cavallo Perin,¹ and Gabriella Gruden¹

OBJECTIVE—Cannabinoid receptor 1 (CB1) is localized in the central nervous system and in peripheral tissues involved in energy metabolism control. However, CB1 receptors are also expressed at low level within the glomeruli, and the aim of this study was to investigate their potential relevance in the pathogenesis of proteinuria in experimental type 1 diabetes.

RESEARCH DESIGN AND METHODS—Streptozotocin-induced diabetic mice were treated with *N*-(piperidin-1-yl)-5-(4-iodophenyl)-1-(2,3-dichlorophenyl)-4-methyl-1H-pyrazole-3-carboxamide (AM251), a selective CB1-receptor antagonist, at the dosage of 1 mg · kg⁻¹ · day⁻¹ via intraperitoneal injection for 14 weeks. Urinary albumin excretion was measured by enzyme-linked immunosorbent assay. CB1 receptor expression was studied by immunohistochemistry, immunoblotting, and real-time PCR. Expression of nephrin, podocin, synaptopodin, and zonula occludens-1 (ZO-1) was assessed by immunofluorescence and real-time PCR. Fibronectin, transforming growth factor-β1 (TGF-β1), and connective tissue growth factor (CTGF) mRNA levels were quantitated by real-time PCR.

RESULTS—In diabetic mice, the CB1 receptor was overexpressed within the glomeruli, predominantly by glomerular podocytes. Blockade of the CB1 receptor did not affect body weight, blood glucose, and blood pressure levels in either diabetic or control mice. Albuminuria was increased in diabetic mice compared with control animals and was significantly ameliorated by treatment with AM251. Furthermore, CB1 blockade completely prevented diabetes-induced downregulation of nephrin, podocin, and ZO-1. By contrast overexpression of fibronectin, *TGF-β1*, and *CTGF* in renal cortex of diabetic mice was unaltered by AM251 administration.

CONCLUSIONS—In experimental type 1 diabetes, the CB1 receptor is overexpressed by glomerular podocytes, and blockade of the CB1 receptor ameliorates albuminuria possibly via prevention of nephrin, podocin, and ZO-1 loss. *Diabetes* 59: 1046–1054, 2010

From the ¹Diabetic Nephropathy Laboratory, Department of Internal Medicine, University of Turin, Turin, Italy; the ²Renal Research Laboratory, Fondazione Istituto di Ricovero e Cura a Carattere Scientifico (IRCCS), Ospedale Maggiore Policlinico and Fondazione D'Amico per la Ricerca sulle Malattie Renali, Milan, Italy; the ³MIA Consortium for Image Analysis, Milano Bicocca University, Milan, Italy; and the ⁴Endocannabinoid Research Group, Institute of Biomolecular Chemistry, Pozzuoli, Italy.

Corresponding author: Gabriella Gruden, gabriella.gruden@unito.it.
Received 10 September 2009 and accepted 30 December 2009. Published ahead of print at <http://diabetes.diabetesjournals.org> on 12 January 2010.
DOI: 10.2337/db09-1336.

© 2010 by the American Diabetes Association. Readers may use this article as long as the work is properly cited, the use is educational and not for profit, and the work is not altered. See <http://creativecommons.org/licenses/by-nc-nd/3.0/> for details.

The costs of publication of this article were defrayed in part by the payment of page charges. This article must therefore be hereby marked "advertisement" in accordance with 18 U.S.C. Section 1734 solely to indicate this fact.

Diabetic nephropathy is characterized by increased glomerular permeability to proteins and excessive extracellular matrix accumulation in the mesangium, eventually resulting in glomerulosclerosis and progressive renal impairment (1).

Recently, increasing attention has been paid to the role of podocytes in the pathogenesis of proteinuric conditions (2,3). The slit diaphragm, a junction connecting foot processes of neighboring podocytes, represents the major restriction site to protein filtration (4), and a causal link between loss of slit diaphragm molecules, such as nephrin and podocin, and the onset of proteinuria has been established (5–7). In both human and experimental diabetic nephropathy, there is a reduction in nephrin expression, and studies in patients with microalbuminuria have demonstrated that nephrin downregulation occurs in an early stage of the disease, supporting the hypothesis of a role of nephrin loss in glomerular albumin leakage (8–10). A number of factors, including advanced glycation end products (10), glomerular hypertension (10,11), angiotensin II (10), and inflammatory cytokines (12) have been implicated in the downregulation of slit diaphragm proteins in diabetes, but the precise mechanism is still largely unknown.

The cannabinoid receptor of type 1 (CB1), a G-protein-coupled receptor, is expressed predominantly in the central nervous system (13), but it has been also found in peripheral tissues, such as the liver (14), adipose tissue (15), pancreas (16), and skeletal muscle (17), where it plays a key role in the control of peripheral energy metabolism. A recent study has shown that the CB1 receptor is expressed at a low level within the glomeruli and that CB1 receptor blockade ameliorates proteinuria in an animal model of obesity-induced nephropathy (18). Although in obese animals the antiproteinuric effect of CB1 antagonism is likely related to amelioration of the metabolic profile, the observation that the CB1 receptor is present within the glomeruli raises the hypothesis of a direct effect of signaling through the CB1 receptor on podocytes and possibly on glomerular permeability to proteins.

To assess the role of the CB1 receptor in the pathogenesis of proteinuria in diabetes, we studied glomerular CB1 receptor expression in streptozotocin (STZ)-induced diabetic mice. Furthermore, we tested whether CB1 receptor blockade affects proteinuria and/or expression of slit diaphragm and slit diaphragm-associated proteins in this model.

RESEARCH DESIGN AND METHODS

Materials. All materials were purchased from Sigma-Aldrich (St. Louis, MO) unless otherwise stated.

Drug. *N*-(piperidin-1-yl)-5-(4-iodophenyl)-1-(2,3-dichlorophenyl)-4-methyl-1H-pyrrolo[2,3-*b*]pyridine-3-carboxamide (AM251), a CB1 receptor antagonist, was purchased from Cayman Chemical (Ann Arbor, MI), dissolved in ethanol to a stock concentration of 3 mg/ml, and stored at -80°C . Stock solutions were diluted in 18:1:1 ratio of saline/emulphor-620/absolute ethanol immediately prior to use. AM251 conjugated with 5-carboxytetramethylrhodamine was purchased from Tocris (Bristol, U.K.).

Animals and induction of diabetes. Both housing and care of laboratory animals were in accordance with Italian law (D.L.116/1992). Male C57BL/6J mice from The Jackson Laboratory (Bar Harbor, ME) were maintained on a normal diet under standard animal house conditions. Diabetes was induced in mice, aged 8 weeks and weighing ~ 22 g, by intraperitoneal injection of STZ-citrate buffer (55 mg \cdot kg body $\text{wt}^{-1} \cdot \text{day}^{-1}$) delivered in five consecutive daily doses. Mice sham-injected with sodium citrate buffer were used as controls. Diabetes onset was confirmed by blood glucose levels >250 mg/dl 4 weeks after the first dose of STZ; only animals with glucose levels >250 mg/dl (95%) were included in the study.

Experimental protocol. Animals were divided into the following groups: nondiabetic mice given vehicle ($n = 7$), nondiabetic mice given AM251 ($n = 8$), diabetic mice given vehicle ($n = 11$), and diabetic mice given AM251 ($n = 10$). AM251 was administered daily at the dosage of 1 mg/kg i.p. Mice sham-injected with a mixture 18:1:1 of saline/emulphor-620/absolute ethanol were used as controls. After 14 weeks of experimental diabetes, mice were killed by decapitation. The kidneys were rapidly dissected and weighed. The right kidney was frozen in N_2 and stored at -80°C for mRNA and protein analysis. Half left kidney was fixed in 10% PBS-formalin, then paraffin-embedded for light microscopy; the remaining tissue was embedded in optimal cutting temperature compound and snap-frozen in N_2 . For electron microscopy, 1-mm³ pieces of renal cortex were fixed in 2% glutaraldehyde, 4% paraformaldehyde in phosphate buffer 0.12 mol/l for 4 h at room temperature, postfixed in 1% osmium tetroxide for 2 h, dehydrated in graded ethanol, and embedded in Epon 812.

Metabolic and physiological parameters. Before killing, blood samples were taken via saphenous vein puncture on alert, 4 h-fasted animals, and glucose levels measured using a glucometer (Accucheck; Roche, Milan, Italy). Systolic blood pressure was assessed by tail-cuff plethysmography in prewarmed unanesthetized animals. Urine was collected over 18 h, with each mouse individually housed in a metabolic cage and provided with food and water ad libitum. Urinary albumin concentration was measured by a mouse albumin ELISA kit (Bethyl Laboratories). Creatinine clearance was estimated from serum and urine creatinine concentrations, as determined by high-performance liquid chromatography (19). Glycated hemoglobin was measured in whole blood samples obtained at the time of killing by quantitative immunoturbidimetric latex determination (Sentinel Diagnostic, Milan, Italy). Urinary *N*-acetylglucosamine (NAG) activity was assessed by colorimetric assay (Roche), and results were expressed as urinary NAG activity-to-creatinine ratio.

Immunohistochemistry. After antigen retrieval and blocking, 4- μm kidney paraffin sections were incubated overnight at 4°C with either anti-CB1 (Cayman Chemical) or WT-1 (Santa Cruz Biotechnology, Glostrup, Denmark) primary antibodies; then the specific staining was detected using the labeled streptavidin biotin + system horseradish peroxidase (Dako, Glostrup, Denmark). Sections were examined using an Olympus microscope (Olympus Bx41), digitized with a high-resolution camera (Carl Zeiss, Oberkochen, Germany). A negative control was included in which the primary antibody was preincubated with a control peptide. Hippocampus sections were used as positive control for CB1. The percentage area of staining and the podocyte number/glomerular area were quantified by a computer-aided image analysis system (Axiovision 4.7; Carl Zeiss), where 20 glomeruli and 11 renal tubulo-interstitial fields for each section were analyzed. Evaluations were performed by two independent investigators in a blinded fashion.

Immunofluorescence. Snap-frozen sections (3 μm), fixed in cold acetone and blocked in 3% BSA, were incubated with guinea pig anti-nephrin (Progen Biotechnik, Maaßstraße, Germany), rabbit anti-podocin, anti-synaptopodin (Synaptic System, Gottingen, Germany), or anti-zonula occludens-1 (ZO-1; Zymed Laboratories, San Francisco, CA) primary antibodies. After washing, fluorescein isothiocyanate-conjugated anti-guinea pig (Santa Cruz Biotechnology) and anti-rabbit (Dako) secondary antibodies were added. Sections were examined using an Olympus epifluorescence microscope (Olympus Bx41), digitized with a high-resolution camera (Carl Zeiss). Results were calculated as percentage positively stained tissue within the glomerular tuft. On average, 20 randomly selected hilar glomerular tuft cross-sections were assessed per mouse.

Double immunofluorescence. Double immunofluorescent staining was performed for CB1 and the specific podocyte marker nephrin. After blocking, sections were incubated with an anti-nephrin antibody and washed; then a fluorescein isothiocyanate-conjugated donkey anti-guinea pig antibody was

added. After washing, sections were incubated with a rabbit anti-CB1 antibody for 18 h at 4°C , washed, and overlaid with a biotinylated swine anti-rabbit IgG (Dako) and then with Alexa-555-conjugated streptavidin (Invitrogen, Milan, Italy).

Binding of AM251 to the CB1 receptor was assessed by double fluorescence. After immunostaining for the CB1 receptor, as described above, sections were incubated with the AM251 fluorescent analog at 1 $\mu\text{mol/l}$ concentration for 30 min, then washed, mounted, and visualized by epifluorescence microscopy.

Western blotting. Total kidney was homogenized in radioimmunoprecipitation assay buffer containing 0.5% Nonidet P-40, 0.5% sodium deoxycholate, 0.1% SDS, 10 mmol/l EDTA, and protease inhibitors. Proteins were separated by SDS-PAGE and electrotransferred to nitrocellulose membrane. After blocking in 5% nonfat milk, membranes were incubated with a rabbit anti-CB1 antibody (Calbiochem, Darstadt, Germany) overnight at 4°C . After washing, secondary anti-rabbit horseradish peroxidase-linked (Amersham) antibody was added. Detection was performed using SuperSignal West Femto chemiluminescence substrate (Pierce, Rockford, IL) and visualized on a Gel-Doc system (Bio-Rad). Band intensities were quantified by densitometry. Tubulin was used as internal control.

Quantitative real-time RT-PCR. Total RNA was extracted from the renal cortex using TRIZOL reagent (Invitrogen). Total RNA (1 μg) was reverse transcribed into cDNA using the high-capacity reverse transcription kit (Applied Biosystems, Monza, Italy). *CB1*, nephrin, podocin, *ZO-1*, transforming growth factor- β 1 (*TGF- β 1*), connective tissue growth factor (*CTGF*), and fibronectin mRNA expression was analyzed by TaqMan real-time PCR using predeveloped TaqMan reagents (Applied Biosystems; *CB1*: Mm00432621; nephrin: Mm00497828; podocin: Mm00499929; *ZO-1*: Mm01320537; *TGF- β 1*: Mm00441724; *CTGF*: Mm00515790; fibronectin: Mm01256744). Fluorescence for each cycle was analyzed quantitatively and gene expression normalized relative to the expression of HPRT. Because housekeeping genes ubiquitously expressed in the renal cortex do not control for variations in the glomerular number per specimen or changes in podocyte number (20), *WT-1*, a podocyte-specific gene, was used as endogenous reference for the evaluation of nephrin, podocin, and *ZO-1* mRNA expression.

Podocyte apoptosis. Apoptosis was assessed by the transferase-mediated dUTP nick-end labeling (TUNEL) method using the ApopTag In Situ Apoptosis Detection Kit (Millipore, Billerica, MA). Results were expressed as the number of positive cells per glomerulus in at least 20 random glomeruli. Slides pretreated with 20,000 units/ml DNase were used as positive control.

Glomerular volume. Glomerular cross-sectional area (A_G) was measured in 20 glomerular profiles per mouse using a computerized image analysis system (Axiovision 4.7; Carl Zeiss). The glomerular volume (V_G) was then calculated as $V_G = \beta/K[A_G]^{1.32}$, where $\beta = 1.38$ is the size distributor coefficient and $K = 1.01$ is the shape coefficient for glomeruli idealized as a sphere (21).

Electron microscopy. Ultrathin sections for ultrastructural examination were cut with the Ultracut E Reichert-Jung ultramicrotome, stained with uranylacetate and lead citrate, and examined with the transmission electron microscope Philips CM 10. Microphotographs were taken using a SIS Megaview II digital camera. Mean foot process width (FPW) was assessed as previously described (22,23) (supplementary Materials, available in an online appendix at <http://diabetes.diabetesjournals.org/cgi/content/full/dc09-1336/DC1>).

Data presentation and statistical analysis. Data, presented as means \pm SEM, geometric mean (25th–75th percentile), or fold change over control, were analyzed by Student *t* test or ANOVA, as appropriate. Least significant difference test was used for post hoc comparisons. Values for $P < 0.05$ were considered significant.

RESULTS

Metabolic and physiological parameters in control and diabetic mice. As shown in Table 1, after 14 weeks of diabetes both blood glucose and glycated hemoglobin levels were significantly higher in diabetic than in nondiabetic mice. Furthermore, compared with sham-injected control animals, diabetic mice showed a significant decrease in body weight. Systolic blood pressure was slightly higher in diabetic than in control mice, but this did not reach statistical significance.

Expression of the CB1 receptor in experimental diabetes. To establish whether the CB1 receptor is expressed within the glomeruli and its expression is modulated by diabetes, we studied CB1 expression in kidney sections from both diabetic and control mice by immuno-

TABLE 1
General assessment parameters in each of the study groups

	Nondiabetic	Nondiabetic + AM251	Diabetic	Diabetic + AM251
Body wt (g)	28.71 ± 1.13	29.41 ± 0.56	25.23 ± 0.84*	25.86 ± 0.69*
Blood glucose (mg/dl)	120 ± 5.81	104 ± 12.07	411 ± 36.07†	386 ± 36.64†
Glycated Hb (%)	4.23 ± 0.05	4.40 ± 0.16	12.93 ± 0.32†	12.49 ± 0.24†
sBP (mmHg)	101 ± 3.30	98 ± 3.30	119 ± 10.50	118 ± 3.79
Kidney/body wt	6.62 ± 0.03	6.46 ± 0.19	8.42 ± 0.99	7.34 ± 0.29
AER (μg/18 h)	33.4 (25.1–40.2)	37.5 (12.6–126.4)	336.6 (164.9–778.5)†	153.1 (70.7–298.1)†‡

Data are shown as means ± SE or geometric mean (25th–75th percentile). sBP, systolic blood pressure; AER, albumin excretion rate. * $P < 0.05$ diabetic and diabetic + AM251 vs. nondiabetic and nondiabetic + AM251; † $P < 0.001$ diabetic and diabetic + AM251 vs. nondiabetic and nondiabetic + AM251; ‡ $P < 0.01$ diabetic + AM251 vs. diabetic.

histochemistry. In control animals, only few glomerular cells stained positively for CB1 (Fig. 1A). CB1 protein expression was enhanced in diabetic mice (Fig. 1B) and semiquantitative analysis showed that the percentage positive area was 1.5-fold greater than in the controls (Fig. 1E). Specificity of the antibody binding was confirmed by disappearance of the signal when the antibody was preabsorbed with a 10-fold excess of control peptide. In the tubuli, staining for the CB1 receptor was faint and no differences were observed between control and diabetic mice (nondiabetic: 2.07 ± 0.73 ; diabetic: 2.54 ± 0.32 ; $P =$ not significant) (Fig. 1C and D).

To clarify which glomerular cell type overexpressed the CB1 receptor, double-labeling immunofluorescence was performed in diabetic mice for the detection of both CB1 and nephrin. The CB1 receptor was expressed primarily by glomerular podocytes as the positive staining for nephrin (Fig. 1L) colocalized with CB1 staining (Fig. 1I), resulting in a partial yellow overlap (Fig. 1M and N).

To confirm immunohistochemistry findings with more quantitative techniques, we measured *CB1* mRNA and protein expression in total renal cortex by real-time PCR and immunoblotting. There was a significant two-fold increase in *CB1* mRNA levels in diabetic mice (Fig. 1F) compared with nondiabetic control animals. Immunoblotting showed a band migrating at ~60 kDa, corresponding to the reported molecular weight of CB1 (Fig. 1G), and densitometric analysis demonstrated that CB1 protein expression was significantly increased in the diabetic mice (Fig. 1G and H).

AM251 binding to the CB1 receptor. As shown in Fig. 1O–Q, glomerular staining using a fluorescent AM251 analog overlapped with the immunofluorescent staining for the CB1 receptor, confirming that AM251 binds to the CB1 receptor.

Effect of treatment with AM251 on metabolic and physiological parameters. As shown in Table 1, treatment with AM251 did not affect the degree of glycemic control because both blood glucose and glycated hemoglobin levels were similar in treated and untreated diabetic animals. In addition, in both diabetic and control animals administration of AM251 did not alter body weight. Finally, no differences were observed in systolic blood pressure.

Effect of CB1 receptor blockade on albuminuria, NAG activity, and renal function. After 14 weeks of diabetes, there was a more than 10-fold increase in urinary albumin excretion rate in diabetic compared with nondiabetic animals. Treatment with AM251 did not alter albuminuria in the controls, but induced a significant 50% reduction in albumin excretion rate levels in the diabetic mice (Table 1). Results were similar when they were expressed as urinary albumin/creatinine ratio (nondia-

betic: 146 ± 6.88 ; nondiabetic + AM251: 147.9 ± 33.87 ; diabetic: 2447.5 ± 607.7 ; diabetic + AM251: 806.3 ± 190.5 ; $P < 0.001$ diabetic vs. others). Urinary NAG activity/creatinine ratio, a marker of tubular damage, was slightly increased in diabetic mice compared with controls, although not significantly. In addition, no differences were observed between treated and untreated diabetic mice (nondiabetic: 88.11 ± 8.37 ; nondiabetic + AM251: 93.16 ± 16.52 ; diabetic: 178.13 ± 21.43 ; diabetic + AM251: 180.64 ± 40.86 units/g; $P =$ not significant). Renal function was similar among groups as assessed by measurement of creatinine clearance (nondiabetic: 0.38 ± 0.07 ; diabetic: 0.41 ± 0.1 ; diabetic + AM251: 0.5 ± 0.1 ml/min; $P =$ not significant).

Effect of AM251 on nephrin, podocin, ZO-1, and synaptopodin expression. To clarify the underlying mechanism of the beneficial effect of CB1 blockade on albuminuria, we assessed the effect of treatment with AM251 on the expression of nephrin, podocin, ZO-1, and synaptopodin by immunofluorescence. After 14 weeks of diabetes, there was a significant reduction in nephrin, podocin, and ZO-1 protein expression, and this effect was completely prevented in diabetic mice treated with AM251 (Fig. 2A–F). No significant changes in synaptopodin protein levels were observed among groups (Fig. 2G and H).

We also assessed nephrin, podocin, and *ZO-1* mRNA in total renal cortex from all groups by real-time PCR and found a significant reduction in nephrin, podocin, and *ZO-1* mRNA levels in diabetic compared with control mice. Treatment with AM251 prevented diabetes-induced nephrin and podocin mRNA downregulation (Fig. 3A and B). A similar trend was also observed for *ZO-1*, although it did not reach statistical significance (Fig. 3C).

Effect of CB1 receptor blockade on podocyte injury. To establish whether in diabetic mice treated with AM251, podocyte protein expression was preserved because CB1 blockade prevented podocyte damage, podocyte number, apoptosis, and ultrastructure were assessed by WT-1 staining, TUNEL assay, and electron microscopy, respectively. The number of both WT-1- and TUNEL-positive cells per glomerular cross-sectional area displayed in a podocyte distribution did not differ among groups (Fig. 4) (nondiabetic: 2.0 ± 0.5 ; diabetic: 2.2 ± 0.4 ; nondiabetic + AM251: 2.5 ± 0.3 ; diabetic + AM251: 2.1 ± 0.5 , TUNEL-positive cells per 100 glomeruli; $P =$ not significant). Electron microscopy analysis did not show any evidence of ultrastructural glomerular (Fig. 4A–F) and tubular (Fig. 5G–L) damage in the studied animals. In particular, the normal arrangement of interdigitating foot processes was maintained in all groups, and podocyte foot processes appeared tall and narrow in both treated and untreated diabetic mice (Fig. 5A–F). Furthermore, mean FPW was compara-

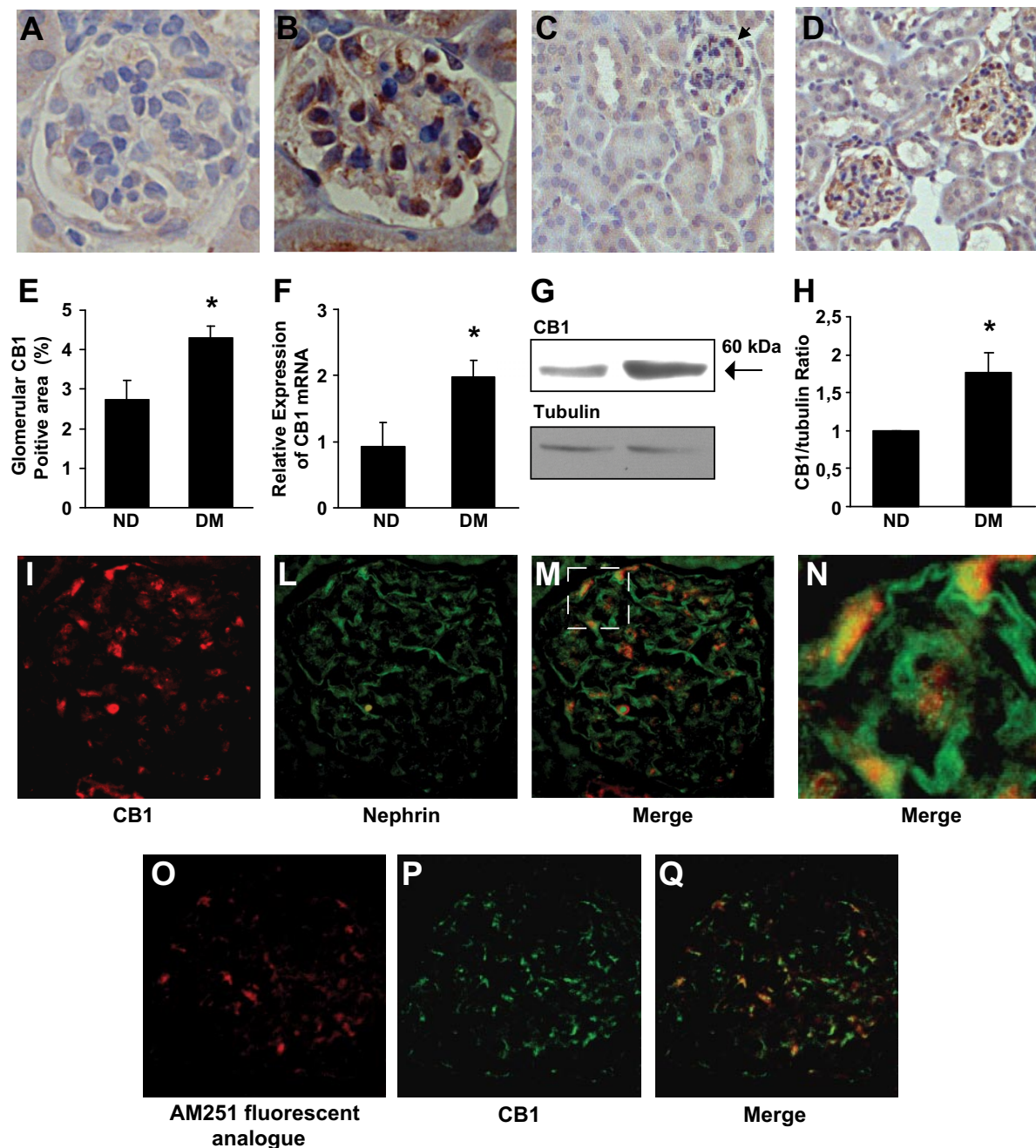


FIG. 1. The CB1 receptor is overexpressed in experimental diabetes. CB1 protein expression was assessed in renal sections from nondiabetic (A and C) and diabetic (B and D) mice by immunohistochemistry as described in the “Research Design and Methods” section (magnification $\times 400$: in A and B; $\times 100$ in C and D). Percentage area of staining for CB1, quantified by a computer-aided image analysis system, is shown for both diabetic and nondiabetic mice ($*P < 0.05$ diabetic vs. nondiabetic) (E). CB1 mRNA levels in renal cortex from both diabetic and nondiabetic mice were measured by real-time PCR and corrected for the expression of the housekeeping gene *HPRT* as described in the “Research Design and Methods” section ($*P < 0.05$ diabetic vs. nondiabetic) (F). CB1 protein expression was assessed by immunoblotting in total protein extracts of renal cortex from diabetic and nondiabetic mice. Tubulin was used as internal control. A representative immunoblot and results of densitometry analyses are shown ($*P < 0.05$ diabetic vs. nondiabetic) (G and H). Double immunofluorescence for CB1 (I) and nephrin (L) performed on diabetic glomeruli showed colocalization of the positive staining, as demonstrated by merging (M). The dashed square in M delimits the area shown at higher magnification in N. Binding of AM251 fluorescent analogue (O) and CB1 immunostaining (P) overlapped in the diabetic glomeruli as shown by merging (Q). (A high-quality digital representation of this figure is available in the online issue.)

ble among groups (nondiabetic: 350 ± 1.33 ; nondiabetic + AM251: 352 ± 1.27 ; diabetic: 375 ± 1.11 ; diabetic + AM251: 364 ± 0.99 nm; $P =$ not significant).

Effect of CB1 blockade on glomerular hypertrophy and early markers of fibrosis. Glomerular volume was significantly increased in diabetic mice compared with control animals and this effect was not altered by treatment with AM251 (nondiabetic: 136 ± 10.33 ; diabetic:

358 ± 19.06 ; nondiabetic + AM251: 127 ± 4.98 ; diabetic + AM251: 369 ± 5.72 μm^3 ; $P < 0.05$ diabetic and diabetic + AM251 vs. nondiabetic).

At electron microscopy, the degree of mesangial expansion and glomerular basement membrane thickening was very mild in diabetic mice, and no major differences were observed among groups (Fig. 4A–D). However, in the renal cortex levels of mRNA encoding for fibronectin, *TGF- β 1*,

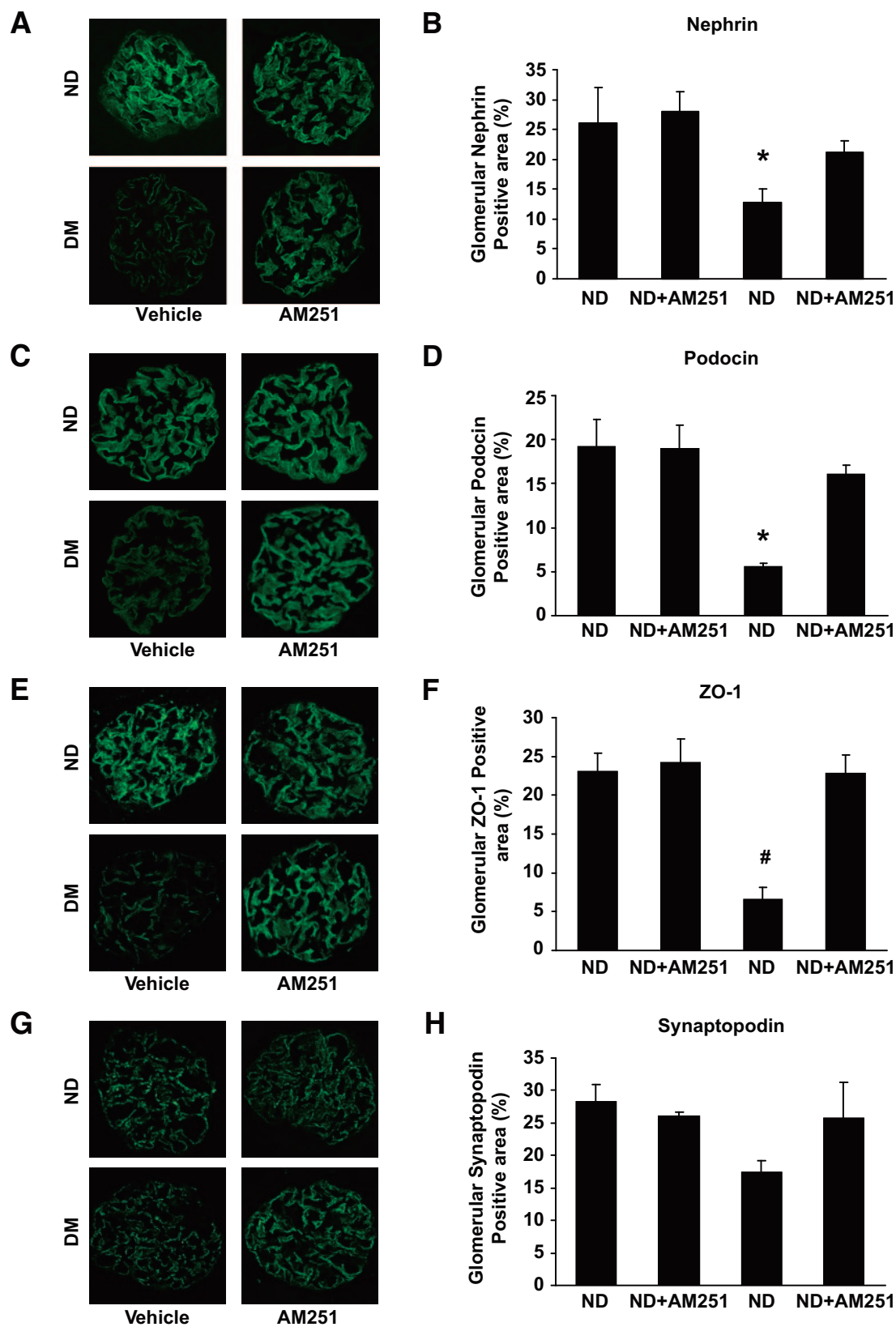


FIG. 2. CB1 blockade abolished downregulation of nephrin, podocin, and ZO-1 protein expression in diabetic mice. Renal cryostatic sections from both diabetic and nondiabetic mice, treated with either vehicle or the CB1 antagonist AM251 for 14 weeks, were stained for nephrin (A), podocin (C), ZO-1 (E), and synaptopodin (G) by immunofluorescence as described in the “Research Design and Methods” section (magnification $\times 400$). Quantification of glomerular staining for nephrin (B), podocin (D), ZO-1 (F), and synaptopodin (H) is shown (* $P < 0.01$ diabetic vs. others; # $P < 0.001$ diabetic vs. others). (A high-quality digital representation of this figure is available in the online issue.)

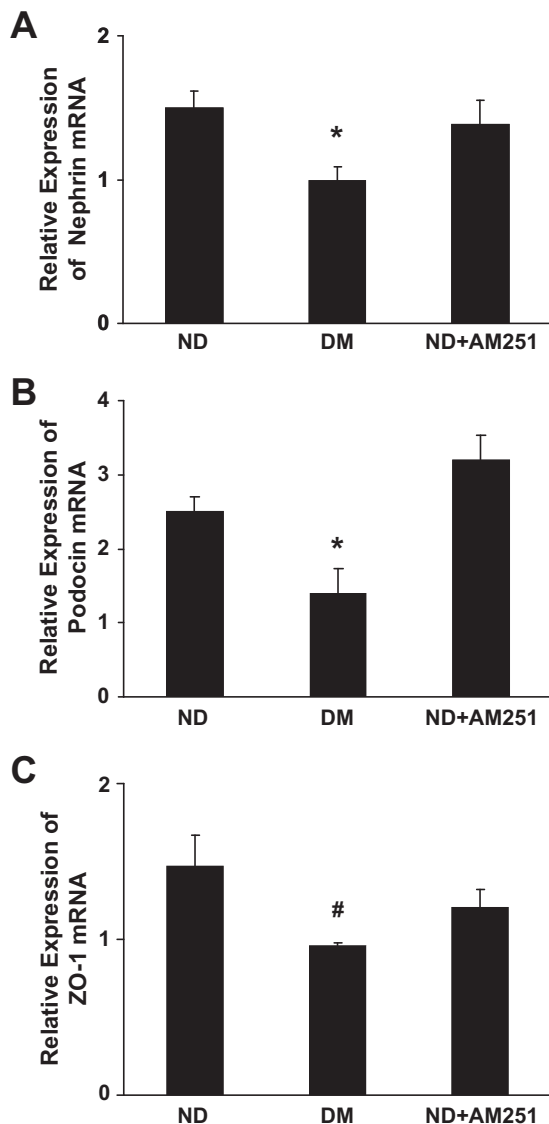


FIG. 3. CB1 blockade prevented diabetes-induced reduction of both nephrin and podocin gene expression. Total RNA was extracted from the renal cortex of nondiabetic and diabetic mice treated with either vehicle (diabetic mice) or the CB1 antagonist AM251 (diabetic + AM251) for 14 weeks. Nephrin (A), podocin (B), and *ZO-1* (C) mRNA levels were measured by real-time PCR and corrected for the expression of *WT-1* as described in the “Research Design and Methods” section (* $P < 0.05$ diabetic vs. nondiabetic and diabetic + AM251; # $P < 0.05$ diabetic vs. nondiabetic).

and *CTGF* were significantly greater in diabetic than in control animals. Treatment of diabetic mice with AM251 did not affect the overexpression of these markers of fibrosis, suggesting that CB1 blockade does not have antifibrotic properties in this model (Figure 6A–C).

DISCUSSION

In this study, we have provided evidence that in experimental diabetes the CB1 receptor is overexpressed within the glomeruli, predominantly by glomerular podocytes. Second, we have shown that blockade of the CB1 receptor with AM251 ameliorates albuminuria and prevents down-regulation of nephrin, podocin, and *ZO-1*. Taken together, these data suggest a role of the CB1 receptor in the pathogenesis of proteinuria in diabetes.

In nondiabetic mice, only a few glomerular cells stained

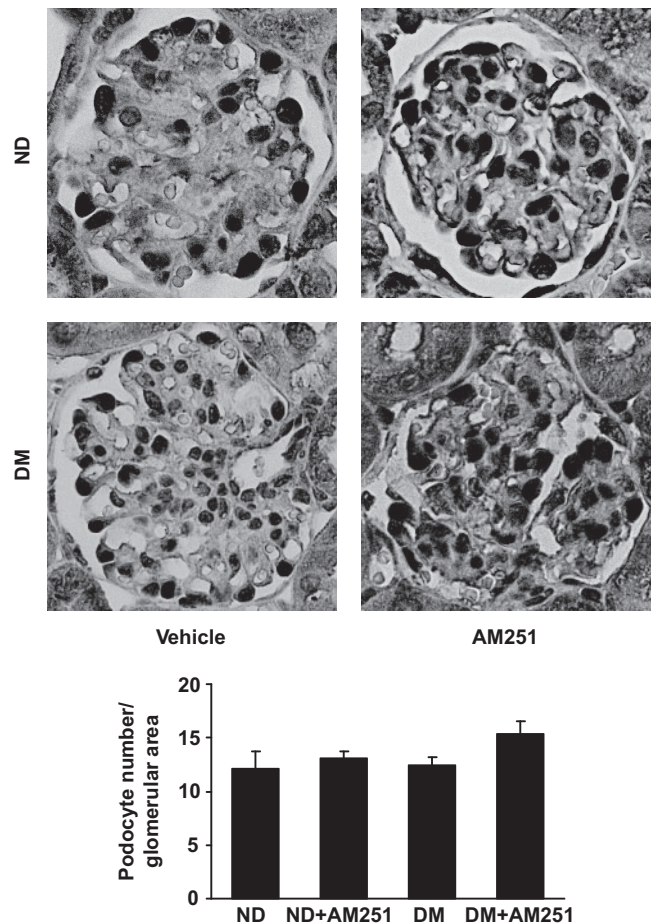


FIG. 4. Podocytes number in diabetic and nondiabetic mice treated with either vehicle or AM251. WT-1 protein expression was assessed by immunohistochemistry in the glomeruli from nondiabetic and diabetic mice treated for 14 weeks with either vehicle or the CB1 receptor antagonist AM251. Quantification of WT-1–positive cells per glomerular area is shown in the graph.

positively for the CB1 receptor, but after 14 weeks of experimental diabetes there was a significant 1.5-fold increase in glomerular CB1 expression. A previous study has shown that the CB1 receptor is expressed at low level in rat kidneys, but no differences in renal CB1 expression were observed between Zucker fatty rats and lean animals (18). Therefore, this is the first evidence of glomerular CB1 overexpression in experimental diabetes and, to our knowledge, in any renal disease.

In agreement with previous data in rat kidneys (18), immunoreactivity for CB1 was predominantly localized to the glomeruli. A faint signal was also detectable in the tubuli, but it was not enhanced in the diabetic mice. Both pattern of staining and colocalization with the podocyte marker nephrin strongly indicate that in diabetic mice the CB1 receptor was primarily overexpressed by glomerular podocytes. This is not surprising because similarities have been reported between podocytes and neurons (24,25), the predominant CB1 receptor–expressing cell type in physiological conditions (13). The underlying mechanism/s of CB1 receptor induction in diabetic podocytes is entirely unknown. However, oxidative stress, which is enhanced in the diabetic glomeruli, is known to induce CB1 receptor expression in other cell types (26).

Consistent with our immunohistochemical data, we found a significant 1.8- to 2-fold increase in CB1 both

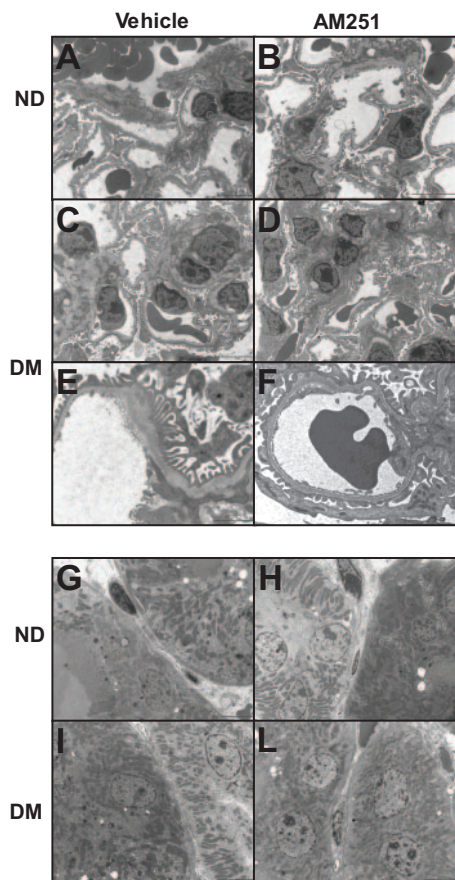


FIG. 5. Transmission electron microscopy analysis. Representative electron microscopy images of glomeruli (*upper panels*) and tubuli (*lower panels*) from nondiabetic (*A, B, G, and H*; magnification $\times 2600$) and diabetic mice (*C, D, I, and J*; magnification $\times 2600$; *E and F*; magnification $\times 6000$) treated for 14 weeks with either vehicle (*A, C, E, G, and I*) or the CB1 receptor antagonist AM251 (*B, D, F, H, and J*). In *A* and *B* the glomerular structure is normal. Glomeruli from diabetic mice (*C* and *D*) display some degree of mesangial expansion, independent of treatment. At higher magnification (*E* and *F*) the podocyte foot processes are regularly shaped and only a minimal irregularity in the thickness of the GBM can be observed in *E*. Tubular structure appears normal in both control and diabetic mice (*G* and *I*) and unaffected by treatment with AM251 (*H* and *J*).

protein and mRNA expression in renal cortex from diabetic mice as assessed by immunoblotting and real-time PCR. Diabetes-induced enhanced transcription of the *CB1* receptor is a potential underlying mechanism as both activator protein 1 (AP-1) and nuclear factor- κ B (27,28), the transcription factors predominantly implicated in the pathogenesis of diabetic nephropathy, have binding sites on the promoter region of the *CB1* receptor gene (29).

To establish whether upregulation of the CB1 receptor in podocytes plays a role in the pathogenesis of proteinuria in diabetes, we studied the effect of treatment with AM251. AM251, a potent and specific CB1 receptor inverse agonist (30–33), is structurally very close to rimonabant, but exhibits better binding affinity and selectivity for the CB1 receptor (33). In our model, selectivity of AM251 binding to the CB1 receptor was indirectly confirmed by colocalization of AM251 and CB1 within the diabetic glomeruli. AM251 was administered daily at the dosage of 1 mg/kg on the basis of previous studies that have proven both efficacy and safety of this dose in mice (34,35). Delivery was via intraperitoneal injection to ensure that all animals were given an equal amount of drug. After 14

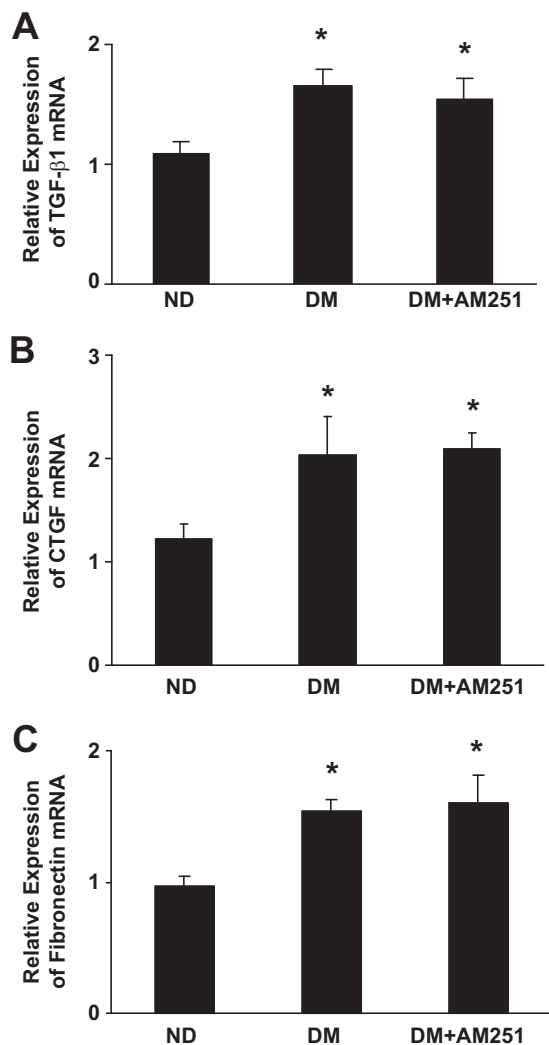


FIG. 6. CB1 blockade did not affect overexpression of fibronectin, TGF- β 1, and CTGF in diabetic mice. Total RNA was extracted from the renal cortex of nondiabetic and diabetic mice treated with either vehicle (diabetic mice) or the CB1 antagonist AM251 (diabetic + AM251) for 14 weeks. *TGF- β 1* (*A*), *CTGF* (*B*), and fibronectin (*C*) mRNA levels were measured by real-time PCR and corrected for the expression of the gene housekeeping *HPRT* as described in the “Research Design and Methods” section ($*P < 0.05$ diabetic and diabetic + AM251 vs. nondiabetic).

weeks of diabetes, there was a 10-fold increase in albuminuria in diabetic mice compared with controls. Treatment with AM251 induced a significant 50% reduction in albuminuria in diabetic mice, supporting the hypothesis that signaling through the CB1 receptor contributes to enhanced glomerular permeability to albumin.

Administration of AM251 did not affect body weight in either diabetic or control mice. This is in agreement with previous reports showing that CB1 blockade prevents weight gain in animals with diet-induced obesity, but is much less efficacious at exerting this effect in lean animals fed a standard diet (36–38). Furthermore, blood glucose levels, glycated hemoglobin, and systolic blood pressure were similar in treated and untreated diabetic mice, consistent with the antiproteinuric effect of CB1 blockade observed in these mice being independent of both metabolic and hemodynamic factors. A significant reduction in proteinuria has been recently reported in obese Zucker fatty rats treated with rimonabant (18); however, in this

model CB1 receptor was not overexpressed in the glomeruli, and the antiproteinuric effect was most likely due to amelioration of the metabolic profile because it was associated with body weight loss and diminution of both blood glucose and lipid levels. In our study, we have purposely chosen an animal model of type 1 diabetes without obesity, insulin resistance, and lipid abnormalities to ensure that the beneficial effects of CB1 blockade were independent of changes in metabolism.

To clarify the mechanism/s of the beneficial effect of AM251, we tested whether CB1 receptor blockade prevents downregulation of podocyte proteins implicated in the maintenance of glomerular permselectivity to proteins. After 14 weeks of diabetes, there was a significant reduction in nephrin, podocin, and ZO-1 both mRNA and protein expression. Treatment with AM251 prevented diabetes-induced downregulation of nephrin, podocin, and ZO-1 protein expression. Results were confirmed by mRNA analysis for both nephrin and podocin, and a similar trend was also observed for *ZO-1*. Loss of slit diaphragm and slit diaphragm-associated proteins has been implicated in the pathogenesis of proteinuria (2); therefore, downregulation of nephrin, podocin, and ZO-1 is a possible mechanism whereby CB1 overexpression may lead to increased glomerular permeability to albumin.

The number of both total and apoptotic podocytes was not increased in diabetic mice. Furthermore, there was no evidence of podocyte foot process effacement at the ultrastructural level or changes in mean FPW. It is, thus, unlikely that levels of nephrin, podocin, and ZO-1 were normal in diabetic mice treated with AM251 because of prevention of podocyte damage. These data also suggest that in early experimental diabetes, downregulation of slit diaphragm proteins precedes the development of podocyte foot process effacement/loss and that podocyte structural damage is not strictly required for the development of proteinuria. Consistent with this view, in nephrin knockout animals proteinuria occurs even in the absence of any defects in the podocyte foot processes (39). The degree of nephrin reduction required for the development of proteinuria is unknown; however, the parallel downregulation of other slit diaphragm proteins is likely to cause a rise in this threshold level (40).

In the diabetic mice, tubular ultrastructure was normal and urinary activity of NAG, a marker of tubular damage, was comparable in treated and untreated mice. Therefore, prevention of tubular injury is not a likely explanation of AM251 antiproteinuric activity. However, we cannot exclude the possibility that at a later stage of experimental diabetes, when severe tubular damage occurs, CB1 blockade may have further beneficial effects due to prevention of tubulointerstitial injury, as previously shown in the Zucker fatty rat model (18).

Glomerular hypertrophy and accumulation of extracellular matrix components, which is mediated predominantly by the prosclerotic cytokines TGF- β 1 and CTGF, are other characteristic features of diabetic nephropathy (1). In our study, after 14 weeks of mild diabetes, C57BL6/J mice, which are relatively resistant to the development of glomerulosclerosis, did not show major ultrastructural abnormalities in the mesangium and the glomerular basement membrane. However, there was a significant increase in both glomerular volume and renal mRNA expression of fibronectin, TGF- β 1, and CTGF in diabetic mice. These diabetes-induced effects were left unchanged by treatment with AM251, indicating failure of CB1 block-

ade in interfering with glomerular hypertrophy and renal fibrogenesis. In animal models of chronic liver injury, blockade of the CB1 receptor decreases fibrosis by lowering hepatic TGF- β 1 expression and reducing accumulation of fibrogenic cells (14). The different effect of CB1 blockade on renal and liver fibrosis is not entirely surprising because the cell types overexpressing the CB1 receptor in liver cirrhosis, namely myofibroblasts and hepatic stellate cells, have much greater profibrotic potential than podocytes. In addition, a tissue-specific effect of CB1 receptor activation cannot be excluded.

In conclusion, our findings may have important implications for diabetic nephropathy in humans. Proteinuria is a characteristic feature of diabetic nephropathy and a key determinant of progression (1). Nephrin is downregulated in early diabetic nephropathy, and this has been implicated in the pathogenesis of the diabetic proteinuria (10). Our data, showing upregulation of CB1 receptors in podocytes and a beneficial effect of AM251 on both albuminuria and nephrin loss, suggest that an elevated CB1 receptor tone (41) is also involved in the pathogenesis of the diabetic proteinuria and identify a new target for therapeutic intervention.

ACKNOWLEDGMENTS

This work was supported by the Compagnia di San Paolo, the Italian Society of Diabetes, the University of Turin (ex-60% grant), and the Piedmont Region Research Grant.

No potential conflicts of interest relevant to this article were reported.

REFERENCES

- Molitch ME, DeFronzo RA, Franz MJ, Keane WF, Mogensen CE, Parving HH, Steffes MW, American Diabetes Association. Nephropathy in diabetes. *Diabetes Care* 2004;27:S79–S83
- Li JJ, Kwak SJ, Jung DS, Kim JJ, Yoo TH, Ryu DR, Han SH, Choi HY, Lee JE, Moon SJ, Kim DK, Han DS, Kang SW. Podocyte biology in diabetic nephropathy. *Kidney Int* 2007;106:S36–S42
- Wolf G, Chen S, Ziyadeh FN. From the periphery of the glomerular capillary wall toward the center of disease: podocyte injury comes of age in diabetic nephropathy. *Diabetes* 2005;54:1626–1634
- Pavenstädt H, Kriz W, Kretzler M. Cell biology of the glomerular podocyte. *Physiol Rev* 2003;83:253–307
- Kestila M, Lenkkeri U, Mannikko M, Lamerdin J, McCready P, Putaala H, Ruotsalainen V, Morita T, Nissinen M, Herva R, Kashtan CE, Peltonen L, Holmberg C, Olsen A, Tryggvason K. Positionally cloned gene for a novel glomerular protein—nephrin—is mutated in congenital nephrotic syndrome. *Mol Cell* 1998;1:572–578
- Beltcheva O, Martin P, Lenkkeri U, Tryggvason K. Mutation spectrum in the nephrin gene (NPHS1) in congenital nephrotic syndrome. *Hum Mutat* 2001;17:368–373
- Route N, Gribouval O, Roselli S, Benessy F, Lee H, Fuchshuber A, Dahan K, Gubler MC, Niaudet P, Antignac C. NPHS2, encoding the glomerular protein podocin, is mutated in autosomal recessive steroid-resistant nephrotic syndrome. *Nat Genet* 2000;24:349–354
- Cooper ME, Mundel P, Boner G. Role of nephrin in renal disease including diabetic nephropathy. *Semin Nephrol* 2002;22:393–398
- Bonnet F, Cooper ME, Kawachi H, Allen TJ, Boner G, Cao Z. Irbesartan normalises the deficiency in glomerular nephrin expression in a model of diabetes and hypertension. *Diabetologia* 2001;44:874–877
- Doublier S, Salvadio G, Lupia E, Ruotsalainen V, Verzola D, Deferrari G, Camussi G. Nephrin expression is reduced in human diabetic nephropathy: evidence for a distinct role for glycated albumin and angiotensin II. *Diabetes* 2003;52:1023–1030
- Langham RG, Kelly DJ, Cox AJ, Thomson NM, Holthöfer H, Zaoui P, Pinel N, Cordonnier DJ, Gilbert RE. Proteinuria and the expression of the podocyte slit diaphragm protein, nephrin, in diabetic nephropathy: effects of angiotensin converting enzyme inhibition. *Diabetologia* 2002;45:1572–1576
- Tarabra E, Giunti S, Barutta F, Salvadio G, Burt D, Deferrari G, Gambino R, Vergola D, Pinach S, Cavallo Perin P, Camussi G, Gruden G. Effect of the

- MCP-1/CCR2 system on nephrin expression in streptozotocin-treated mice and human cultured podocytes. *Diabetes* 2009;58:2109–2118.
13. Kano M, Ohno-Shosaku T, Hashimoto-dani Y, Uchigashima M, Watanabe M. Endocannabinoid-mediated control of synaptic transmission. *Physiol Rev* 2009;9:309–380
 14. Teixeira-Clerc F, Julien B, Grenard P, Tran Van Nhieu J, Deveaux V, Li L, Serriere-Lanneau V, Ledent C, Mallat A, Lotersztajn S. CB1 cannabinoid receptor antagonism: a new strategy for the treatment of liver fibrosis. *Nat Med* 2006;12:671–676
 15. Roche R, Hoareau L, Bes-Houtmann S, Gontherier MP, Laborde C, Baron JF, Haffaf Y, Cesari M, Festy F. Presence of the cannabinoid receptors, CB1 and CB2, in human omental and subcutaneous adipocytes. *Histochem Cell Biol* 2006;126:177–187
 16. Nakata M, Yada T. Cannabinoids inhibit insulin secretion and cytosolic Ca²⁺ oscillation in islet beta-cells via CB1 receptors. *Regul Pept* 2008;145:49–53
 17. Cavuoto P, McAinch AJ, Hatzinikolaou G, Janovska A, Game P, Wittert GA. The expression of receptors for endocannabinoids in human and rodent skeletal muscle. *Biochem Biophys Res Comm* 2007;364:105–110
 18. Janiak P, Poirier B, Bidouard JP, Cadrouvele C, Pierre F, Gouraud L, Barbosa I, Dedio J, Maffrand JP, Le Fur G, O'Connor S, Herbert JM. Blockade of cannabinoid CB1 receptor improves renal function, metabolic profile, and increased survival of obese Zucker rats. *Kidney Int* 2007;72:1345–1357
 19. Dunn SR, Qi Z, Bottinger EP, Breyer MD, Sharma K. Utility of endogenous creatinine clearance as a measure of renal function in mice. *Kidney Int* 2004;65:1959–1967
 20. Schmid H, Henger A, Cohen CD, Frach K, Gröne HJ, Schlöndorff D, Kretzler M. Gene expression profiles of podocyte-associated molecules as diagnostic markers in acquired proteinuric diseases. *J Am Soc Nephrol* 2003;14:2958–2966
 21. Weibel ER. Stereological methods. In: *Practical Methods for Biological Morphometry*. London, U.K., Academic, 1979, p. 51–57
 22. Pagtalunan ME, Rasch R, Rennke HG, Meyer TW. Morphometric analysis of effects of angiotensin II on glomerular structure in rats. *Am J Physiol* 1995;268:F82–F88
 23. Deegens JK, Dijkman HB, Borm GF, Steenbergen EJ, van den Berg JG, Weening JJ, Wetzels JF. Podocyte foot process effacement as a diagnostic tool in focal segmental glomerulosclerosis. *Kidney Int* 2008;74:1568–1576
 24. Kobayashi N, Gao SY, Chen J, Saito K, Miyawaki K, Li CY, Pan L, Saito S, Terashita T, Matsuda S. Process formation of the renal glomerular podocyte: is there common molecular machinery for processes of podocytes and neurons? *Anat Sci Int* 2004;79:1–10
 25. Rastaldi MP, Armelloni S, Berra S, Calvaresi N, Corbelli A, Giardino LA, Li M, Wang GQ, Fornasieri A, Villa A, Heikkilä E, Soliymani R, Boucherot A, Cohen CD, Kretzler M, Nitsche A, Ripamonti M, Malgaroli A, Pesaresi M, Forloni GL, Schlöndorff D, Holthofer H, D'Amico G. Glomerular podocytes contain neuron-like functional synaptic vesicles. *FASEB J* 2006;20:976–978
 26. Wei Y, Wang X, Wang L. Presence and regulation of cannabinoid receptors in human retinal pigment epithelial cells. *Mol Vis* 2009;15:1243–1251
 27. Ahn JD, Morishita R, Kaneda Y, Kim HJ, Kim YD, Lee HJ, Lee KU, Park JY, Kim YH, Park KK, Chang YC, Yoon KH, Kwon HS, Park KG, Lee IK. Transcription factor decoy for AP-1 reduces mesangial cell proliferation and extracellular matrix production in vitro and in vivo. *Gene Ther* 2004;11:916–923
 28. Yang B, Hodgkinson A, Oates PJ, Millward BA, Demaine AG. High glucose induction of DNA-binding activity of the transcription factor NFκB in patients with diabetic nephropathy. *Biochim Biophys Acta* 2008;1782:295–302
 29. Börner C, Höllt V, Kraus J. Activation of human T cells induces upregulation of cannabinoid receptor type 1 transcription. *Neuroimmunomodulation* 2007;14:281–286
 30. Hodadah H, Marcantoni A, Comunanza V, Carabelli V, Carbone E. L-type channel inhibition by CB1 cannabinoid receptors is mediated by PTX-sensitive G proteins and cAMP/PKA in GT1–7 hypothalamic neurons. *Cell Calcium* 2009;46:303–312
 31. Liu Q, Bhat M, Bowen WD, Cheng J. Signaling pathways from cannabinoid receptor-1 activation to inhibition of N-methyl-D-aspartic acid mediated calcium influx and neurotoxicity in dorsal root ganglion neurons. *J Pharmacol Exp Ther* 2009;331:1062–1070
 32. Pertwee RG. Inverse agonism and neutral antagonism at cannabinoid CB1 receptors. *Life Sci* 2005;76:1307–1324
 33. Lan R, Liu Q, Fan P, Lin S, Fernando SR, McCallion D, Pertwee R, Makriyannis A. Structure-activity relationships of pyrazole derivatives as cannabinoid receptor antagonists. *J Med Chem* 1999;42:769–776
 34. Mathes CM, Ferrara M, Rowland NE. Selection of a palatable dietary option is not preferentially reduced by cannabinoid CB1 receptor antagonist AM251 in female C57Bl/6J mice. *Pharmacol Biochem Behav* 2009;94:119–123
 35. de Filippis D, Iuvone T, d'Amico A, Esposito G, Steardo L, Herman AG, Pelckmans PA, de Winter BY, de Man JG. Effect of cannabidiol on sepsis-induced motility disturbances in mice: involvement of CB receptors and fatty acid amide hydrolase. *Neurogastroenterol Motil* 2008;20:919–927
 36. Nogueiras R, Veyrat-Durebex C, Suchanek PM, Klein M, Tschöp J, Caldwell C, Woods SC, Wittmann G, Watanabe M, Liposits Z, Fekete C, Reizes O, Rohner-Jeanrenaud F, Tschöp MH. Peripheral, but not central, CB1 antagonism provides food intake-independent metabolic benefits in diet-induced obese rats. *Diabetes* 2008;57:2977–2991
 37. Serrano A, Del Arco I, Javier Pavón F, Macías M, Perez-Valero V, Rodríguez de Fonseca F. The cannabinoid CB1 receptor antagonist SR141716A (Rimonabant) enhances the metabolic benefits of long-term treatment with oleoylethanolamide in Zucker rats. *Neuropharmacology* 2008;54:226–234
 38. Vickers SP, Webster LJ, Wyatt A, Dourish CT, Kennett GA. Preferential effects of the cannabinoid CB1 receptor antagonist, SR 141716, on food intake and body weight gain of obese (fa/fa) compared to lean Zucker rats. *Psychopharmacology* 2003;167:103–111
 39. Kalluri R. Proteinuria with and without renal glomerular podocyte effacement. *J Am Soc Nephrol* 2006;17:2383–2389
 40. Koziell A, Grech V, Hussain S, Lee G, Lenkkeri U, Tryggvason K, Scambler P. Genotype/phenotype correlations of NPHS1 and NPHS2 mutations in nephrotic syndrome advocate a functional inter-relationship in glomerular filtration. *Hum Mol Genet* 2002;11:379–388
 41. Di Marzo V. Targeting the endocannabinoid system: to enhance or reduce? *Nat Rev Drug Discov* 2008;7:438–455